

# Time-Resolved Vibrational Structures of the Triplet Sublevel Emission of Pd(2-thpy)<sub>2</sub>

J. Schmidt,<sup>†</sup> H. Wiedenhofer,<sup>†</sup> A. von Zelewsky,<sup>‡</sup> and H. Yersin<sup>\*,†</sup>

*Institut für Physikalische und Theoretische Chemie, Universität Regensburg, D-93040 Regensburg, Germany, and Institut de Chimie Inorganique et Analytique, Université de Fribourg, CH-1700 Fribourg, Switzerland*

*Received: March 14, 1994; In Final Form: August 23, 1994*<sup>®</sup>

Time-resolved phosphorescence spectra from the lowest electronic triplet of Pd(2-thpy)<sub>2</sub> (with 2-thpy<sup>−</sup> = ortho-C-deprotonated form of 2-(2-thienyl)pyridine) (see the inset of Figure 2) are presented. The complex was isolated in a Shpol'skii matrix to obtain high resolution. The emitting triplet lies at  $18\,418 \pm 1\text{ cm}^{-1}$  (electronic origin). Its zero-field splitting is less than  $1\text{ cm}^{-1}$  and could not be resolved optically. However, at 1.3 K, when the spin–lattice relaxation is slow compared to the emission lifetimes of the sublevels (130, 235, 1200 μs), the individual sublevels emit independently. Thus, by time-resolved spectroscopy it is possible to separate a fast-decaying emission spectrum from a slow-decaying one. A highlight of this investigation is that these spectra exhibit different vibrational satellite structures. This shows that different spin–orbit coupling mechanisms (direct spin–orbit coupling and Herzberg–Teller coupling) govern the radiative deactivation of the sublevels. In particular, it is found that specific vibrational modes couple very selectively to individual sublevels. For example, the  $528\text{ cm}^{-1}$  mode couples only to the slow-decaying sublevel. Thus, these optically well resolvable vibrational satellites display directly properties of the individual sublevels, which are unresolvable by conventional optical spectroscopy. This effect is observed for the first time for transition metal complexes.

## Introduction

The extensive studies of photophysical and photochemical properties of transition metal complexes with organic ligands during the past 20 years were stimulated by possible applications, especially in photocatalytic processes like solar energy conversion.<sup>1–3</sup> These are related in many cases to the properties of the lowest excited electronic states. Moreover, there is substantial scientific interest to develop a better understanding of these compounds, especially since they exhibit a series of electronic and vibronic properties which are found neither in pure organic molecules nor in simple transition metal compounds with metal centered transitions. Valuable information about the nature of the excited states is obtained from highly resolved emission and excitation spectra as well as from emission decay properties. This was demonstrated for the well-known [Ru(bpy)<sub>3</sub>]<sup>2+</sup> and other polypyridine complexes.<sup>4–7</sup> Cyclometalated complexes form a related class of compounds.<sup>2,6,8</sup> Recently, one representative, the Pd(2-thpy)<sub>2</sub> complex (with 2-thpy<sup>−</sup> = ortho-C-deprotonated form of 2-(2-thienyl)pyridine, see the inset in Figure 2), has been studied in detail.<sup>2,6,8–12</sup> By using the Shpol'skii<sup>13</sup> matrix isolation technique it was possible to obtain spectra which were more than a hundred times better resolved<sup>11</sup> than in glassy matrices. Thus, the lowest electronic origin (of triplet character) and a rich vibrational satellite structure could be resolved. For a better understanding of the electronic and vibronic properties of the title compound it is of great interest to obtain more information about the three triplet sublevels. They are split by the zero-field splitting (zfs), which is due to both magnetic dipole–dipole interactions between the two electron spins and spin–orbit coupling mainly induced by the metal ion.<sup>14–16</sup> The value of the splitting depends strongly on the type of transition involved. For example, for a metal-to-ligand charge transfer (MLCT) transition one finds values up to  $\approx 200\text{ cm}^{-1}$  (e.g. [Os(bpy)<sub>3</sub>]<sup>2+</sup><sup>4–7</sup>), while for a transition of mainly ligand-centered  $\pi$ – $\pi^*$  character the zfs may be similar to that in organic

molecules, where it is on the order of  $0.1\text{ cm}^{-1}$  (e.g. [Rh(bpy)<sub>3</sub>]<sup>2+</sup><sup>15,16</sup> and the title compound<sup>11</sup>). By application of conventional optical spectroscopy it is not possible to resolve the sublevels with such a small splitting. However, the sublevels generally emit (nearly) independently at 1.3 K due to the fact that the spin–lattice relaxation rates between them are very small at this temperature. This is also found for the title compound.<sup>11</sup> Further, the emission lifetimes of the individual sublevels are found to be substantially different. Thus, it should be possible to record emission spectra of individual sublevels by use of time-resolved spectroscopy. Indeed, the method is extremely successful as will be demonstrated in this paper for the first time for transition metal complexes. In this way, it can be shown that the radiative decay mechanisms are very characteristic with respect to the different sublevels and the vibrational modes.

## Experimental Section

The preparation<sup>10</sup> of Pd(2-thpy)<sub>2</sub> and application of the Shpol'skii matrix technique<sup>11</sup> is described elsewhere. The final concentration of the chromophore in the matrix was  $\approx 10^{-5}\text{ mol/L}$ . The measurements were mainly performed at 1.3 K. This temperature was achieved by pumping off He in a Leybold-Heraeus BBK 100 cryostat. As excitation source a nitrogen laser was used (Lambda Physik M1000,  $\lambda_{\text{ex}} = 337.1\text{ nm}$ , pulse width  $\approx 3\text{ ns}$ , repetition rate 100 Hz). To avoid sample heating, the exciting laser pulses were attenuated by filters. The optical setup for recording the spectra is described elsewhere.<sup>17</sup> Decay curves were registered with a fast multiscaler (minimum dwell time 5 ns/channel) combined with a multichannel data processor (CMTE 7885 TOF/MCS and MCD/PC). Time-resolved emission spectra were recorded with a gated photon counter (Stanford Research Systems, Model SR 400). The preamplified photomultiplier output pulses were connected to the input of two independent counters of the gated photon counter. Each counter was separately delayed and gated. A trigger pulse synchronously started the exciting laser and the counter. Each counter was activated after its individual delay time  $t$  and stopped after its individual gate time  $\Delta t$  (active window). The counters

<sup>†</sup> Universität Regensburg.

<sup>‡</sup> Université de Fribourg.

<sup>®</sup> Abstract published in *Advance ACS Abstracts*, November 15, 1994.

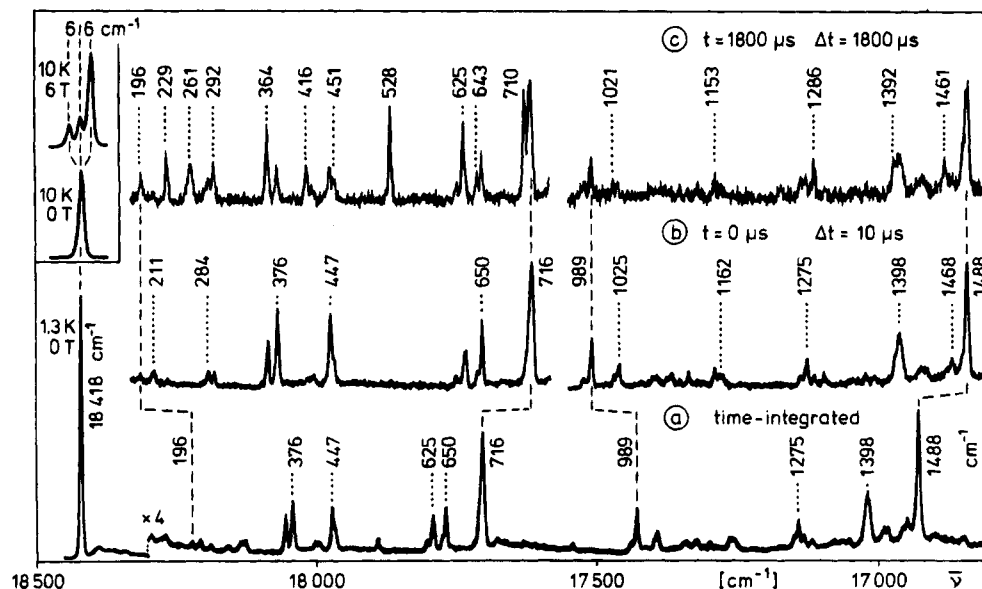


**Figure 1.** Emission spectra of Pd(2-thpy)<sub>2</sub> in an *n*-octane Shpol'skii matrix at 1.3 K (concentration 10<sup>-5</sup> mol/L). (a) Time-integrated emission. (b) Time-resolved emission, delay time  $t = 0 \mu\text{s}$ , time window  $\Delta t = 10 \mu\text{s}$ . (c) Time-resolved emission, delay time  $t = 1800 \mu\text{s}$ , time window  $\Delta t = 1800 \mu\text{s}$ . The energies of the vibrational satellites are specified relative to the electronic origin at 18 418 cm<sup>-1</sup>. The inset shows the splitting of the electronic origin under magnetic field of 6 T at 10 K, taken from ref 18. Note that the cm<sup>-1</sup> scales of (a) are different compared to (b), (c) as well as compared to the inset. The intensities of the different spectra are not comparable.

accumulated data over repetitive count periods until a preset number of trigger pulses was reached. The two counters were read out by a computer via the serial interface and subsequently the detection wavenumber was changed to a new position, and the cycle was started again.

## Results and Discussion

**Time-Integrated Emission.** Figure 1a shows the emission spectrum measured at  $T = 1.3 \text{ K}$  of Pd(2-thpy)<sub>2</sub> in an *n*-octane Shpol'skii matrix, where the chromophores are well isolated due to the low concentration of 10<sup>-5</sup> mol/L. The linewidths of the different peaks are about 3 cm<sup>-1</sup>, which is more than a hundred times smaller than found in glassy matrices. This spectrum represents the usual, time-integrated highly resolved emission. The dominating peak at the position of highest energy ( $\bar{\nu} = 18\,418 \pm 1 \text{ cm}^{-1}$ ) is assigned to the electronic origin, corresponding to the transition between the lowest triplet and the singlet ground state.<sup>11</sup> At zero magnetic field the splitting of this triplet state (zfs) is less than the spectral resolution (1 cm<sup>-1</sup>) of our instrumentation. However, recent ODMR measurements indicate that the zfs is of the order of 0.1 cm<sup>-1</sup>.<sup>11</sup> The triplet character of this electronic state is demonstrated by the splitting of about 12 cm<sup>-1</sup> into three components under application of a magnetic field of 6 T (see the inset of Figure 1 and ref 18). Further, it could be shown<sup>11</sup> that the emitting triplet has to be classified as ligand centered of  $\pi-\pi^*$  character with relatively small MLCT admixtures. The very rich satellite structure is assigned to transitions into vibrational levels of the electronic ground state. It has also been shown that the corresponding vibrational energies are very similar to those of the excited triplet state. Moreover, the vibrational satellite structures do not show any dominating Franck-Condon progression. Thus, it is possible to conclude on very similar ground-state and excited-state equilibrium positions and potential hypersurfaces.<sup>11</sup> The time-integrated zero-field spectrum gives neither detailed information about the individual sublevels nor their specific radiative deactivation properties. This holds also for the sublevels, split under high magnetic field, due to the magnetic-field induced mixing of the corresponding wave functions.<sup>19,20</sup> However, time-resolved spectra, as discussed below, will supply the required information.

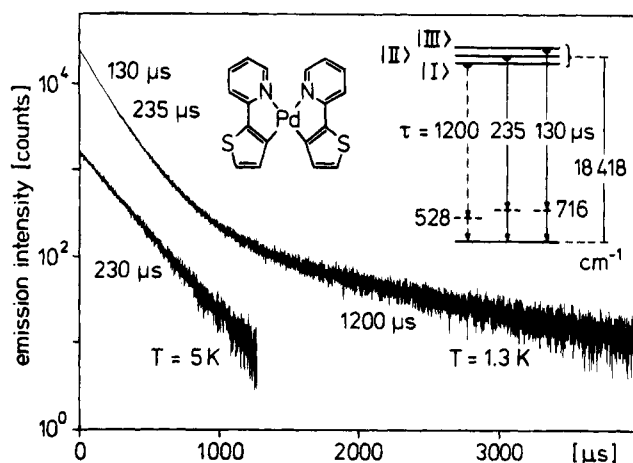


**Figure 2.** Decay curve of Pd(2-thpy)<sub>2</sub> in an *n*-octane Shpol'skii matrix at 1.3 and 5 K recorded on the electronic origin at 18 418 cm<sup>-1</sup> ( $\lambda_{\text{ex}} = 337.1 \text{ nm}$ ). The insets show the structure of the title compound and an energy level scheme. The transitions depicted in this scheme are representative and indicate the selectivity of vibrational coupling of the different triplet sublevels. The order of the sublevels is not known.

**Time-Resolved Emission.** Population of the triplet sublevels is achieved by pulsed excitation of a singlet ( $\lambda_{\text{ex}} = 337.1 \text{ nm}$ ) followed by fast intersystem crossing to the sublevels. The intersystem crossing rates are spin-dependent. Therefore, in the case of pulsed excitation, the initial population of each sublevel is proportional to the intersystem crossing rate to each sublevel and usually a nonequilibrium population of the sublevels results (spin polarization).<sup>21</sup> The subsequent emission decay measured at 18 418 cm<sup>-1</sup> (electronic origin) at 1.3 K is shown in Figure 2. The decay curve is best fitted by three exponentials, corresponding to the emission from three sublevels, |I>, |II>, |III>. (This designation of the sublevels does not indicate an energy order, see also the inset of Figure 2.) One finds two short-living components with lifetimes of  $\tau_{\text{II}} = 235 \pm 15 \mu\text{s}$  (0.38) and  $\tau_{\text{III}} = 130 \pm 10 \mu\text{s}$  (0.54) and a relatively long-living one with  $\tau_{\text{I}} = 1200 \pm 50 \mu\text{s}$  (0.08). (The normalized time-integrated intensity of the specific decay component is given in parentheses.) These fit parameters were obtained by carrying out weighted nonlinear least-squares fits according to the

Marquardt<sup>22</sup> method. With the given fit values we found well randomly distributed residuals with a normalized  $\chi^2 = 1.08$ . (This very careful fit leads to slightly modified values compared to the ones given in ref 11.) We also tested a number of simulations with different initial guesses to fit the experimental decay curve by a sum of two exponentials. However, the residuals showed obvious deviations from random distributions. Thus, it is concluded that a two-exponential model does not adequately describe the observed decay while the proposed model with three exponentials is successful. Moreover, this is expected when comparing the decay behavior with the one of triplets of organic compounds, where usually three components are observed at low temperature.<sup>21,23</sup>

All three decay times are relatively short compared to the lifetime of the free ligand [H(2-thpy):  $\tau(77\text{ K}) = 34\text{ ms}^9$ ], showing that spin-orbit coupling is more efficient in the metal complex than in the pure ligand. This can be explained by a relatively small admixture of MLCT character (with its d-orbital contribution) to the ligand-centered  $\pi-\pi^*$  transition.<sup>2,6,11</sup>

The three sublevels of the title compound are emissive and at 1.3 K the spin-lattice relaxation rates between the sublevels are considerably smaller than the decay rates. The decay curve at the electronic origin is a superposition of the individual decay characteristics of the (nearly) independently emitting sublevels. At 5 K the decay is monoexponential with  $\tau = 230 \pm 10\text{ }\mu\text{s}$  (Figure 2). It is concluded that a temperature increase leads to a strong increase of the spin-lattice relaxation rates by phonon-induced processes<sup>24</sup> and thus to a fast equilibration among the sublevels. The observed monoexponential decay indicates that spin-lattice relaxation is much faster at 5 K than the shortest decay. Using the individual lifetimes of the sublevels, one can determine a "high temperature" mean value  $\tau_{\text{mean}} = 3(1/\tau_{\text{I}} + 1/\tau_{\text{II}} + 1/\tau_{\text{III}})^{-1} = 235 \pm 20\text{ }\mu\text{s}$ . (The derivation of this expression is given, for example, in ref 23.) This mean value lies very close to the measured lifetime at 5 K.

The decay curve at 1.3 K (Figure 2) shows two distinct time regions. In the short-time region the emissions from |II> and |III> dominate and after a delay of about 1600  $\mu\text{s}$  the monoexponential decay of |I> is mainly observed. Thus, it is expected that the spectra of the two fast-decaying sublevels are separable from the slow-decaying level by time-resolved spectroscopy.

Figure 1b shows the time-resolved spectrum registered with no delay with respect to the exciting laser pulse ( $t = 0\text{ }\mu\text{s}$ ) and integrated over a time window  $\Delta t = 10\text{ }\mu\text{s}$ , while Figure 1c reproduces the spectrum with  $t = 1800\text{ }\mu\text{s}$  and a subsequent window of  $\Delta t = 1800\text{ }\mu\text{s}$ . These two spectra differ significantly. It is clearly seen that a series of vibrational satellites grows in with time. For example, vibrational modes at 229, 261, 416, 528, and 710  $\text{cm}^{-1}$  couple *only* to the slow-decaying sublevel (bold-faced in the first column of Table 1). Other satellites increase in their relative intensities with time, e.g., at 364, 625, 1286, and 1461  $\text{cm}^{-1}$ . Therefore, they are important for the deactivation from |I>, but they are also present in the fast-decaying spectrum from |II> and |III>. The two types of modes which exhibit increasing relative intensities with time are summarized in the first column of Table 1. Most of these modes are IR-active (Table 1, third column). On the other hand, several satellites in the fast-decaying spectrum reduce their relative intensities with time, e.g., at 211, 376, 716, and 1488  $\text{cm}^{-1}$ . These are important for the two fast-decaying sublevels |II> and |III>. They are summarized in the second column of Table 1.

Figure 1 shows that the time-integrated spectrum is mainly determined by the fast-decaying transitions (compare Figure 1, a and b) while the information about the slow-decaying sublevel |I> is very poor in the time-integrated spectrum (e.g., see the

**TABLE 1: Vibrational Satellites ( $\text{cm}^{-1}$ ) to the Electronic Origin at  $184 \pm 1\text{ cm}^{-1}$  of  $\text{Pd}(\text{2-thpy})_2$  from Time-Resolved Emission Spectra Compared to IR Data<sup>a</sup>**

emission (1.3 K)		IR (300 K) <sup>c</sup>
rel intensity <sup>b</sup> increase with time	rel intensity <sup>b</sup> decrease with time	
196 m		191 w
	211 m	215 w
<b>229 m</b>		229 s
<b>261 m</b>		265 s
	284 m	
292 m		
364 s		359 w
<b>416 m</b>	376 s	413 s
	424 w	422 w
	447 s	445 w
451 w		455 w
<b>528 s</b>		528 w
625 s		623 w
643 w		642 s
	650 s	
<b>710 s</b>	716 vs <sup>d</sup>	713 m
	989 s	720 m
1021 w		985 s
	1025 m	1022 w
1153 w		1155 vs
	1162 w	
	1275 m	1276 s
1386 m		
1392 m		
	1398 s	1398 s
1461 m		1464 w
	1468 w	
1481 w		1481 vs
	1488 vs <sup>d</sup>	

<sup>a</sup> vs = very strong. s = strong. m = medium. w = weak. <sup>b</sup> Relative intensity is defined as the ratio of the emission intensity of a specific vibrational satellite to the corresponding time-resolved total vibrational emission intensity. (Compare Figure 1b to 1c.) <sup>c</sup> IR spectrum measured at room temperature in KBr and polyethylene pellets, respectively, on a Nicolet 60 SX FT-IR spectrometer (resolution 4  $\text{cm}^{-1}$ ). <sup>d</sup> Weak progression forming mode (from ref 11). In bold-face type: Selective coupling to sublevel |I>.

229, 416, and 528  $\text{cm}^{-1}$  satellites). Thus, it can be concluded that the fast-decaying sublevels carry most of the total emission intensity.

The most intense satellites in the fast-decaying spectrum (716 and 1488  $\text{cm}^{-1}$ , Figure 1b) are members of Franck-Condon progressions, although with very small Huang-Rhys factors (see ref 11). The occurrence of such progressions to the electronic origin(s) allows to conclude on totally symmetric vibrational modes.<sup>25</sup> These are mainly active in the intense electronic transitions from the sublevels |II> and |III> to the ground state. The relatively high allowedness of these transitions can only be explained by an appreciable singlet admixture through direct first order spin-orbit coupling into |II> and |III> (e.g., see ref 25). The change of the intensity distribution of the vibrational satellites, when comparing the fast-decaying spectrum (Figure 1b) to the slow-decaying one (Figure 1c), indicates that different radiative deactivation mechanisms are effective. This change is displayed, for example, in the 528  $\text{cm}^{-1}$  satellite, which is in the slow-decaying spectrum by a factor of 40–50 more important than in the fast-decaying one (normalized to the 716  $\text{cm}^{-1}$  Franck-Condon mode). This behavior—the long lifetime and the change of the vibrational satellite structure—suggests that the radiative decay of sublevel |I> is controlled by vibronic perturbation mechanisms (Herzberg-Teller coupling)<sup>25</sup> and that direct spin-orbit coupling is much less important. A similar

behavior is also found for the radiative deactivation of the lowest sublevels of Pt(2-thpy)<sub>2</sub><sup>6,26</sup> and [Os(bpy)<sub>3</sub>]<sup>2+</sup>.<sup>19</sup> In particular, the modes coupling selectively to sublevel |I> (229, 261, 416, 528, 710 cm<sup>-1</sup>) represent very interesting candidates for investigations of the dynamics of spin–lattice relaxation processes by use of time-resolved emission spectroscopy.

All vibrational satellites, which are found in the fast-decaying spectrum are also found in the slow-decaying one. Thus, they may couple to both, the fast and the slow-decaying sublevels. However, it is also possible that they result from a residual spin–lattice relaxation even at 1.3 K.

The vibrational satellite structures of the two fast decaying sublevels |II> and |III> could not be separated, since the decay times are very similar (130, 235 μs). Moreover, it is possible that both fast-decaying sublevels couple to the same vibrations. Such a situation has been found to occur in Pt(2-thpy)<sub>2</sub>, where the electronic origins corresponding to the different triplet sublevels and the corresponding emission spectra are optically resolvable due to a total zfs of 16 cm<sup>-1</sup>.<sup>26</sup>

## Conclusion

Highly resolved and time-resolved emission spectra of Pd(2-thpy)<sub>2</sub> allow a detailed discussion of the vibrational satellite structure(s) in the phosphorescence from the lowest excited triplet. Despite the fact that the electronic origins of the different sublevels are optically unresolvable, different vibrational satellite spectra were obtained by time resolution at 1.3 K. At this temperature the triplet sublevels emit (nearly) independently, since spin–lattice relaxation rates between the sublevels are very much smaller than the decay rates to the singlet ground state. From the time-resolved emission spectra it is concluded that direct spin–orbit coupling dominates the radiative deactivation of the fast-decaying sublevels |II> and |III>, while vibronic spin–orbit coupling is important for the slow-decaying sublevel |I>. Several modes couple selectively to this sublevel |I>. Therefore, the corresponding vibronic satellites represent interesting candidates for an optical investigation of dynamics of spin–lattice relaxation processes.

**Acknowledgment.** The authors gratefully acknowledge financial funding of the Deutsche Forschungsgemeinschaft and the Verband der Chemischen Industrie.

## References and Notes

- (1) O'Regan, B.; Grätzel, M. *Nature* **1991**, 353, 737.
- (2) Maestri, M.; Balzani, V.; Deuschel-Cornioley, C.; von Zelewsky, A. *Adv. Photochem.* **1992**, 17, 1.
- (3) Yersin, H.; Vogler, A., Eds. *Photochemistry and Photophysics of Coordination Compounds*; Springer Verlag: Berlin, 1987. Yersin, H., Ed. *Electronic and Vibronic Spectra of Transition Metal Complexes I. Topics in Current Chemistry*; Springer Verlag: Berlin, 1994; Vol. 171.
- (4) Yersin, H.; Braun, D.; Hensler, G.; Gallhuber, E. In *Vibronic Processes in Inorganic Chemistry*; Flint, C. D., Ed.; Kluwer: Dordrecht, The Netherlands, 1989; p 195.
- (5) Huber, P.; Yersin, H. *J. Phys. Chem.* **1993**, 97, 12705.
- (6) Yersin, H.; Huber, P.; Wiedenhofer, H. *Coord. Chem. Rev.*, **1994**, 132, 35.
- (7) Braun, D.; Huber, P.; Wudy, J.; Schmidt, J.; Yersin, H. *J. Phys. Chem.* **1994**, 98, 8044.
- (8) Balzani, V.; Maestri, M.; Melandri, A.; Sandrini, D.; Chassot, L.; Cornioley-Deuschel, C.; Jolliet, P.; Maeder, U.; von Zelewsky, A. In *Photochemistry and Photophysics of Coordination Compounds*; Yersin, H., Vogler, A., Eds.; Springer Verlag: Berlin, **1987**; p 71.
- (9) Maestri, M.; Sandrini, D.; Balzani, V.; von Zelewsky, A.; Jolliet, P. *Helv. Chim. Acta* **1988**, 71, 134.
- (10) Jolliet, P. Thesis No. 926, University of Freiburg, Switzerland, 1987.
- (11) Yersin, H.; Schützenmeier, S.; Wiedenhofer, H.; von Zelewsky, A. *J. Phys. Chem.* **1993**, 97, 13496.
- (12) Becker, D.; Wiedenhofer, H.; Schmidt, J.; Yersin, H. *Book of Abstracts; 8<sup>th</sup> International Conference on Photochemical Conversion and Storage of Solar Energy*; Interlaken (Switzerland); Calzaferri, G., Ed.; 1994; p 477.
- (13) Shpol'skii, E. V. *Sov. Phys. Usp. (Engl. Transl.)* **1960**, 3, 372.
- (14) Miki, H.; Shimada, M.; Azumi, T.; Brozik, J. A.; Crosby, G. A. *J. Phys. Chem.* **1993**, 97, 11175.
- (15) Westra, J.; Glasbeek, M. *J. Lumin.* **1992**, 53, 92.
- (16) Kamyshny, A. L.; Suisalu, A. P.; Aslanov, L. A. *Coord. Chem. Rev.* **1992**, 117, 1.
- (17) Stock, M.; Yersin, H. *Chem. Phys. Lett.* **1976**, 40, 423.
- (18) Schützenmeier, S. Thesis, Universität Regensburg, 1992.
- (19) Braun, D.; Hensler, G.; Gallhuber, H.; Yersin, H. *J. Phys. Chem.* **1991**, 95, 1067.
- (20) Gallhuber, E.; Hensler, G.; Yersin, H. *J. Am. Chem. Soc.* **1987**, 109, 4818.
- (21) El-Sayed, M. A. In *Excited States, Vol. I*; Lim, E. C., Ed.; Academic Press: New York, 1974; p 35.
- (22) Demas, J. N. *Excited States Lifetime Measurements*; Academic Press: New York, 1983; p 89.
- (23) Tinti, D. S.; El-Sayed, M. A. *J. Chem. Phys.* **1971**, 54, 2529.
- (24) Scott, P. L.; Jeffries, C. D. *Phys. Rev.* **1962**, 127, 32.
- (25) Albrecht, A. C. *J. Chem. Phys.* **1963**, 38, 354.
- (26) Wiedenhofer, H.; Schützenmeier, S.; Yersin, H.; von Zelewsky, A. *J. Phys. Chem.*, submitted for publication.